

Peak Age of Information Optimization of Slotted Aloha

Dewei Wu, Wen Zhan, Xinghua Sun, Bingpeng Zhou and Jingjing Liu

School of Electronics and Communication Engineering, Shenzhen Campus of Sun Yat-sen University

Email: wudw5@mail2.sysu.edu.cn, {zhanw6, sunxinghua, zhoubp3, liujj77}@mail.sysu.edu.cn

Abstract—The timeliness of information is of capital importance for numerous Internet of Things (IoT) services. To improve the information freshness in large-scale distributed IoT systems, this paper focuses on the Peak Age of Information (PAoI) optimization of slotted Aloha networks. Specifically, by assuming the first-come-first-served (FCFS) service discipline and Bernoulli packet arrival model, the mean PAoI is characterized and then optimized by either individually tuning the channel access probability or jointly tuning the channel access probability and packet arrival rate of each sensor. The explicit expressions of optimal parameter settings and the corresponding minimum PAoI are obtained, based on which the age-throughput tradeoff is evaluated. The analysis is verified by simulations. It is found that in the massive access scenarios, the minimum PAoI linearly increases with the network scale in both individual optimization and joint optimization cases, while the latter attains a lower increasing rate, better age performance, and less throughput loss.

Index Terms—Age of information, slotted Aloha, channel access probability, packet arrival rate.

I. INTRODUCTION

The information freshness is crucial for many real-time Internet of Things (IoT) applications, such as environmental detection, dynamic system control, and e-health, where fast and accurate system responses are vital. To characterize the timeliness of information, a new metric called Age-of-Information (AoI) is proposed in [1], which measures the time elapsed since the last received packet was generated. As the key metric to assess the “freshness” of information, how to characterize and optimize the AoI performance of the network has attained extensive attention.

As the most representative distributed random access protocol, slotted Aloha is especially suitable for large-scale IoT systems, and has been applied in many IoT commercial solutions such as NB-IoT. In slotted Aloha, sensors with non-empty queues would transmit the packet in each time slot with a certain probability. As such, the channel contention process and the network performance shall crucially depend on the packet arrival rate (i.e., the sampling rate in the context of

the information update system [2]) and the channel access probability of each sensor.

For decades, extensive works have been done on optimizing the performance of slotted Aloha by properly selecting the packet arrival rate and the channel access probability, where the classical metrics, such as throughput and delay, were considered [3]–[5]. However, the search for the optimal parameter configuration has long been known as notoriously difficult, especially when the inherent bi-stable behavior problem is considered. That is, the Aloha network may have two steady-state points (i.e., the limiting probability of successful transmissions) and may drop to the lower one, on which the network performance is poor. As such, numerous works have been done on characterizing the bi-stable region of Aloha networks, which is found to be determined by various system parameters including the packet arrival rate and the channel access probability [4], [5].

Apart from the classical performance metrics, the information timeliness metric, AoI, of Aloha networks also has gained significant attention recently [6]–[13]. To push the age performance to the limit, the generate-at-will traffic model, where sensors generate new samples whenever they decide to transmit, has been widely used [7]–[10]. In [7], the average AoI of slotted Aloha was characterized and optimized by properly choosing the channel access probability. [8] considered the multi-channel Aloha network, and optimized the age performance via joint access control and resource allocation. To make the best use of each update transmission, threshold-based random access schemes were proposed, in which channel access request of a sensor is permitted only if the information age exceeds a predetermined threshold [9], [10]. Yet, the generate-at-will traffic model is not in line with many practical IoT services such as smart grid, where the updates come into the data queue periodically or stochastically. With stochastic packet arrivals, however, the bi-stable behavior of Aloha should be considered, with which how to characterize the age performance remains largely unexplored.

For age performance optimization, based on the periodic status update model, [11] derived the average AoI and peak AoI for a real-time status update IoT system with state-dependent slotted Aloha, and further evaluated the optimal update interval. On the other hand, based on the Bernoulli packet arrival model with a fixed packet arrival rate, [12], [13] proposed age-based thinning schemes, in which the optimal transmission probabilities were searched based on an iterative algorithm. The excessively high complexity makes this scheme

This work was supported in part by the National Key Research and Development Program of China (2019YFE0114000), in part by the National Natural Science Foundation of China (62001524, 62001526, 62174181), in part by the Shenzhen Science and Technology Program (Grant No. RCBS20210706092408010 and Grant No. 2021A04), in part by the Natural Science Foundation of Guangdong Province under Grant 2021A1515012021, and in part by the Guangdong Engineering Technology Research Center for Integrated Space-Terrestrial Wireless Optical Communication.

inapplicable to practical IoT networks with low-cost sensors. Meanwhile, besides the channel access probability, the packet arrival rate can also be a tunable system parameter. Another question naturally arises: How to jointly select the packet arrival rate and channel access probability of each sensor for the age performance optimization of slotted Aloha, especially when the bi-stable behavior is considered?

To address the above open issue, in this paper, we consider a slotted Aloha network where each sensor is equipped with a unit-size buffer. The Peak AoI (PAoI)¹, which represents the maximum value of AoI achieved just before an update is received, will be the focus of this paper. By extending the analysis in [4], we take the bi-stable behavior of slotted Aloha into account and obtain the explicit expression of mean PAoI. The optimal backoff parameters for PAoI optimization are carefully selected such that the network would not fall into the bi-stable region, avoiding the risk of dropping to the lower steady-state point. In specific, our contributions are summarized as follows:

- *Individual optimization*: By assuming that the packet arrival rate is fixed, we minimize PAoI by optimally tuning the channel access probability. It is found that the optimal channel access probability for PAoI minimization is the same as the one for access delay minimization.
- *Joint optimization*: When the packet arrival rate can be tuned, we minimize PAoI by jointly tuning the packet arrival rate and channel access probability. The analysis shows that with joint optimization, both the packet arrival rate and channel access probability decrease with the number of sensors, while the corresponding minimum PAoI increases linearly with the number of sensors.
- *Age-throughput tradeoff*: The age-throughput tradeoff is further evaluated in both individual optimization and joint optimization cases. It is found that with individual optimization, there is no throughput performance loss only if the packet arrival rate is large. On the other hand, with joint optimization, the throughput performance loss remains at 2%.

The remainder of our paper is organized as follows. The preliminary analysis of steady-state points and PAoI is presented in Section II. Both individual optimization and joint optimization for minimizing PAoI are addressed in Section III. Concluding remarks are summarized in Section IV.

II. SYSTEM MODEL AND PRELIMINARY ANALYSIS

Consider a slotted Aloha network containing n sensors and one common server. The arrival process of packets follows Bernoulli distribution and each sensor can buffer at most one data packet. Assume that all the sensors are synchronized and can access the channel only at the beginning of a time slot, and each transmission occupies one time slot. The packets generated by sensors are transmitted over a noiseless channel, and each packet can be successfully transmitted when there is no concurrent transmission from other sensors.

¹The primary motivation for using PAoI as the age metric is that one can characterize its stationary distribution using standard methods in queueing theory [14]. The analysis in this paper can be further extended to incorporate other age metrics, such as the average AoI.

In this article, the first-come-first-served (FCFS) service discipline is adopted, so the newly arrived packet will be dropped out if the buffer is full. Assume that with probability $\lambda \in (0, 1]$, each sensor performs the sampling operation at the beginning of each time slot for generating a new packet (i.e., update). When the buffer is non-empty, the sensor will access the channel in each time slot with probability q until the packet is successfully transmitted.

A. Steady-state Points

Let p denote the steady-state probability of successful transmission of each packet. Note that a discrete-time Markov process has been established in [4] for characterizing the behavior of head-of-line (HoL) packets of each sensor, based on which it was obtained

$$p = \exp\left(\frac{-\hat{\lambda}q}{\lambda + pq}\right), \quad (1)$$

where $\hat{\lambda} = n\lambda$ is the aggregate input rate. The above equation shows that p is determined by the number of sensors n , the arrival rate λ and the channel access probability q . According to (1), the network steady-state points can then be calculated.

The analysis in [4] reveals that the network has either two steady-state points, i.e., the desired steady-state point p_L and the undesired steady-state point p_A with $p_L > p_A$, or one steady-state point p_L , depending on whether it operates at the bi-stable region \mathcal{B} or mono-stable region \mathcal{M} , where

- **Bi-stable region** $\mathcal{B} = \{(n, q, \lambda) | n > \frac{4}{q}, \lambda_1 < \lambda < \lambda_2\}$, in which the network has two different steady-state points p_A and p_L . The boundary λ_1 and λ_2 are given by Eq.(7-8) in [4], i.e.,

$$\begin{cases} \lambda_1 = \frac{2}{n\left(1 - \frac{2}{nq} - \sqrt{1 - \frac{4}{nq}}\right) \cdot \exp\left(\frac{2}{1 - \sqrt{1 - \frac{4}{nq}}}\right)} \\ \lambda_2 = \frac{2}{n\left(1 - \frac{2}{nq} + \sqrt{1 - \frac{4}{nq}}\right) \cdot \exp\left(\frac{2}{1 + \sqrt{1 - \frac{4}{nq}}}\right)} \end{cases} \quad (2)$$

- **Mono-stable region** $\mathcal{M} = \bar{\mathcal{B}}$, in which the network has only one steady-state point p_L .

B. Peak Age of Information

This paper focuses on the PAoI of slotted Aloha networks. For illustration, Fig. 1 depicts the evolution of AoI $\Delta(t)$ over time t , where t_i denotes the time instance at which i^{th} packet arrives and t'_i denotes the time instance that i^{th} packet is successfully transmitted, $i \in \{1, 2, \dots\}$. Note that due to the finite buffer size, some packets are dropped and their corresponding t'_i are not exist. As only successfully-transmitted packets contribute to the age performance, we use subscript k to indicate the successfully-transmitted packets and refer to them as informative packets [15], [16].

As Fig. 1 illustrates, the AoI grows over time. When a packet is successfully received, AoI reduces to the time elapsed since the generation of the delivered packet. Therefore, $\Delta(t) = t - u(t)$, $t \in \{1, 2, \dots\}$, where $u(t) = \max\{t_i | 0 <$

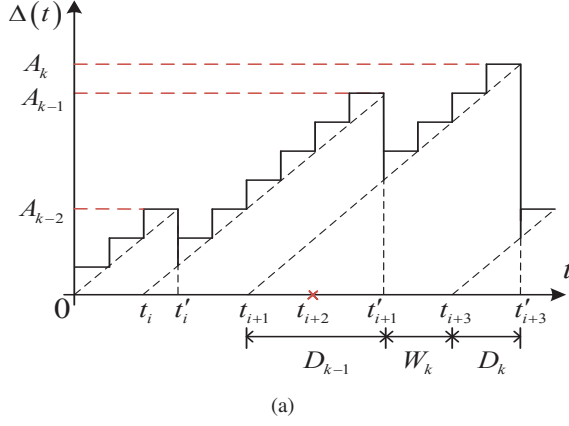


Fig. 1. AoI evolution traces of a sensor.

$t'_i < t\}$. The PAoI, denoted by A_k , is the AoI achieved immediately before receiving the k^{th} packet. Then the mean PAoI A can be defined as

$$A = \lim_{T \rightarrow \infty} \sup \frac{\sum_{t=1}^T \Delta(t) \mathbf{1}\{\Delta(t+1) \leq \Delta(t)\}}{\sum_{t=1}^T \mathbf{1}\{\Delta(t+1) \leq \Delta(t)\}}. \quad (3)$$

According to the service discipline FCFS, we can see from Fig. 1 that the packet arrivals at t_{i+2} is dropped because of the full buffer. The age performance only relies on the packet which arrives when the buffer is empty, i.e., the i^{th} packet, the $i+1^{th}$ packet and the $i+3^{th}$ packet in Fig. 1. Accordingly, upon the successful reception of the k^{th} packet, the PAoI A_k can be written as

$$A_k = D_{k-1} + W_k + D_k, \quad (4)$$

where

- $D_k = t'_k - t_k$ is the access delay of the k^{th} informative packet, i.e., the time interval from the arrival of k^{th} informative packet when the buffer is empty until its successful transmission.
- $W_k = t_k - t'_{k-1}$ is the idle period, which is the time interval from the successful transmission of $k-1^{th}$ informative packet until the arrival of the next packet.

Let us derive the expression of PAoI. The analysis in [17] has revealed that the mean access delay is given by

$$E[D] = \frac{1}{qp}. \quad (5)$$

Since the arrival process of packets follows Bernoulli distribution with parameter λ , and the departure of $i-1^{th}$ successfully transmitted packet as well as the arrival of a new packet can occur at the same time, we can have the mean length of the idle period as

$$E[W] = \frac{1}{\lambda} - 1. \quad (6)$$

Finally based on (4)–(6), we can obtain the mean PAoI as

$$A = \frac{2}{qp} + \frac{1}{\lambda} - 1. \quad (7)$$

C. Problem Definition

In this paper, our objective is to minimize the mean PAoI A via optimally tuning the channel access probability q

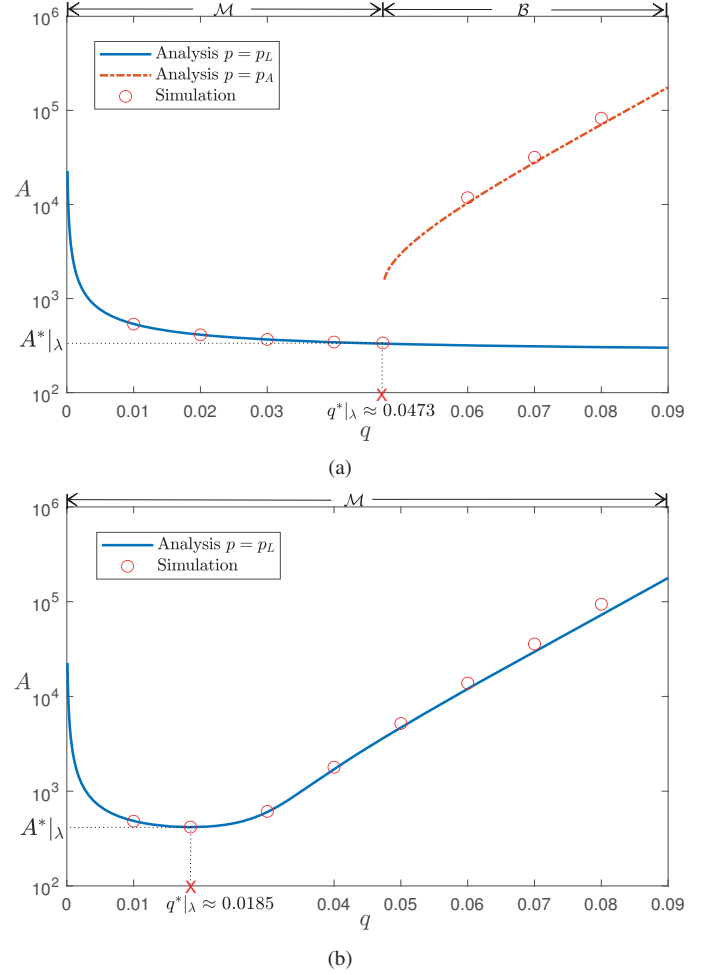


Fig. 2. PAoI A versus the channel access probability q , $n = 100$. (a) $\lambda = 0.004$. (b) $\lambda = 0.008$.

and the packet arrival rate λ . Note that the channel access probability is a MAC layer parameter that can be dynamically adjusted, while the packet arrival rate is usually determined by the sensing strategy, which is an application-dependent parameter. For instance, in smart grid, the sensor usually sends a packet every 15 minutes [18]. Accordingly, we consider two optimization problems. The first one is the individual optimization problem, where the network aims at minimizing the PAoI A by individually tuning q given the packet arrival rate λ , i.e.,

$$A^*|_{\lambda} = \min_{0 < q \leq 1} A. \quad (8)$$

If the packet arrival rate λ can be tuned, then we have the joint optimization problem, where the PAoI is minimized by jointly tuning q and λ , i.e.,

$$A^* = \min_{0 < q \leq 1, 0 < \lambda \leq 1} A. \quad (9)$$

In the following section, we will address the above optimization problems.

III. PAOI OPTIMIZATION

A. Individual Optimization

The following theorem presents the optimal channel access probability $q^*|_{\lambda}$ that minimizes the PAoI when the packet

arrival rate λ and the number of sensors² n are given.

Theorem 1. Given the aggregate input rate $\hat{\lambda}$, the minimum PAoI is given by

$$A^*|_{\lambda} = \begin{cases} 2e \cdot n - \frac{1}{\lambda} - 1 & \hat{\lambda} > \hat{\lambda}_0, \\ \frac{n(-2\mathbb{W}_{-1}(-\frac{\sqrt{n\lambda}}{2})-1)}{2\mathbb{W}_{-1}^2(-\frac{\sqrt{n\lambda}}{2})p_L^*} + \frac{1}{\lambda} - 1 & \text{otherwise,} \end{cases} \quad (10)$$

which is achieved when the channel access probability is set to

$$q^*|_{\lambda} = \begin{cases} \frac{\lambda}{n\lambda - e^{-1}} & \hat{\lambda} > \hat{\lambda}_0, \\ \frac{4\mathbb{W}_{-1}^2(-\frac{\sqrt{n\lambda}}{2})}{n(-2\mathbb{W}_{-1}(-\frac{\sqrt{n\lambda}}{2})-1)} & \text{otherwise,} \end{cases} \quad (11)$$

where $\hat{\lambda}_0 \approx 0.48$ and p_L^* is the non-zero root of the following equation

$$p_L^* = \exp\left(\frac{-4n\lambda\mathbb{W}_{-1}^2(-\frac{\sqrt{n\lambda}}{2})}{4p_L^*\mathbb{W}_{-1}^2(-\frac{\sqrt{n\lambda}}{2}) + n\lambda(-2\mathbb{W}_{-1}(-\frac{\sqrt{n\lambda}}{2})-1)}\right). \quad (12)$$

Proof. Given the aggregate input rate $\hat{\lambda}$, it can be seen from (5) and (7) that PAoI minimization is equivalent to mean access delay minimization. Therefore, the optimal channel access probability for minimizing the mean access delay can also minimize the PAoI. The optimal channel access probability has been obtained in [17], as shown by (11). The minimum PAoI can then be obtained by substituting (11) into (1) and (7). \square

Theorem 1 reveals that the optimal channel access probability $q^*|_{\lambda}$ is $\frac{\lambda}{n\lambda - e^{-1}}$ when the aggregate input rate is larger than $\hat{\lambda}_0$. Otherwise, $q^*|_{\lambda}$ should be set to be $\frac{4\mathbb{W}_{-1}^2(-\frac{\sqrt{n\lambda}}{2})}{n(-2\mathbb{W}_{-1}(-\frac{\sqrt{n\lambda}}{2})-1)}$, which is the root of $\lambda = \lambda_1$ for avoiding the network falls into the bi-stable region \mathcal{B} , where λ_1 is given in (2).

Fig. 2 depicts how the PAoI A varies with the channel access probability q with a setting that the number of sensors $n = 100$ and the aggregate input rate $\hat{\lambda} = 0.4$ or 0.8 . The simulation setting is the same as the system model and thus the details are omitted here. With $\hat{\lambda} = 0.4 \leq \hat{\lambda}_0$, it can be seen from Fig. 2 (a) that the PAoI decreases as q increases when the network stays in mono-stable region \mathcal{M} . When $q > q^*|_{\lambda} \approx 0.047$, the network falls into bi-stable region \mathcal{B} , in which it has two steady-state points, i.e., the desired steady-state point p_L and the undesired steady-state point p_A . Once the network shifts to the undesired steady-state point p_A , the PAoI A rises sharply. To hedge against this case, the optimal channel access probability $q^*|_{\lambda}$ is set to the region boundary, i.e., the root of $\lambda = \lambda_1$. On the other hand, if the aggregate input rate increases to 0.8 , then the network always stays in mono-stable region \mathcal{M} and operates at the desired steady-state point p_L . The minimum PAoI can be achieved when q is set

²Note that the number of sensors should be distinguished from the number of active sensors in existing works [19], [20]. Specifically, the server can keep a record of registered sensors without knowing if they are active or not at each time slot. In contrast, tracking and estimating the time-varying number of active sensors in each time slot can be highly challenging and demanding in large-scale IoT.

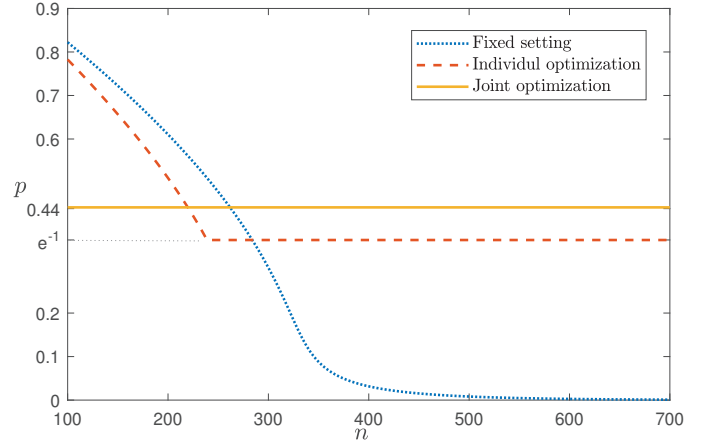


Fig. 3. Steady-state probability of successful transmission p versus n in three different cases, $q = 0.01$, $\lambda = 0.002$.

to $q^*|_{\lambda} = \frac{\lambda}{n\lambda - e^{-1}} \approx 0.018$. The analysis match well with the simulations.

B. Joint optimization

Note that if the packet arrival rate of each device λ can be adjusted, then the network can jointly tune q and λ for PAoI minimization. The following theorem presents the optimal channel access probability q^* and packet arrival rate λ^* for PAoI minimization.

Theorem 2. The minimum PAoI A^* is given by

$$A^* \approx 3.27n - 1, \quad (13)$$

which is achieved when

$$\begin{cases} q^* \approx \frac{4.543}{n}, \\ \lambda^* \approx \frac{0.4395}{n}. \end{cases} \quad (14)$$

Proof. See Appendix A. \square

Theorem 2 reveals that as the number of devices n increases, both the optimal channel access probability q^* and packet arrival rate λ^* should be properly reduced in order to alleviate the contention. Meanwhile, the minimum PAoI A^* linearly increases with n .

Fig. 3 demonstrates how the steady-state point p varies with n in three cases: 1) fixed setting with $\lambda = 0.002$ and $q = 0.01$, 2) individual q optimization with $\lambda = 0.002$ and 3) joint q and λ optimization. It can be seen that with fixed setting, successful transmission probability p decreases with the number of sensors n . With individual tuning, p declines only when n is small and stays at e^{-1} when n is large. With joint optimization, p becomes insensitive to n and always operates at 0.44 .

Recall that existing works on slotted Aloha have revealed that for throughput maximization, the steady-state point p should be at e^{-1} . Accordingly, the above observation reveals that for age performance optimization with joint optimization, where $p = 0.44$, the throughput performance would be sacrificed. To take a closer look at the throughput performance

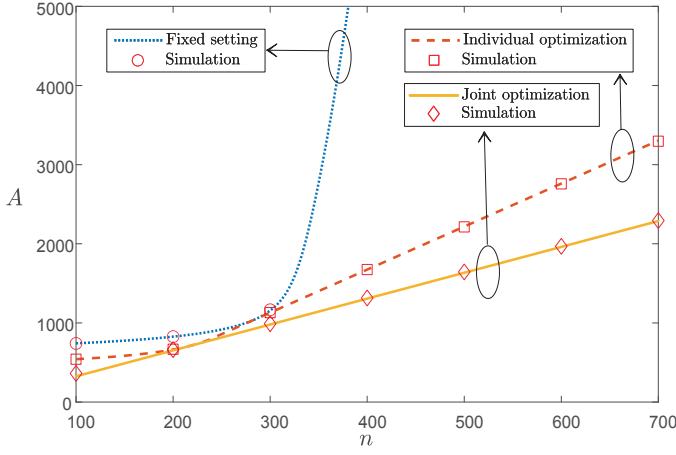


Fig. 4. PAoI A versus n in three different cases, $q = 0.01$, $\lambda = 0.002$.

loss, let us revisit the network throughput of slotted Aloha with single buffer size, which is denoted by λ_{out} and given by [4]

$$\lambda_{out} = \frac{n\lambda qp}{\lambda + qp}. \quad (15)$$

With individual optimization, the throughput can be obtained as follows by combining (11) and (15).

$$\lambda_{out}^{q=q^*|_{\lambda}} = \begin{cases} e^{-1} & \hat{\lambda} > \hat{\lambda}_0, \\ \frac{4n\lambda p_L^* \mathbb{W}_{-1}^2(-\frac{\sqrt{n\lambda}}{2})}{n\lambda(-2\mathbb{W}_{-1}(-\frac{\sqrt{n\lambda}}{2})-1)+4p_L^* \mathbb{W}_{-1}^2(-\frac{\sqrt{n\lambda}}{2})} & \text{otherwise,} \end{cases} \quad (16)$$

where p_L^* is given in (12). We can see from (16) that when the packet arrival rate is large, i.e., $\hat{\lambda} > \hat{\lambda}_0 \approx 0.48$, there is no throughput performance loss, as $\lambda_{out}^{q=q^*|_{\lambda}} = e^{-1}$. Otherwise, the throughput performance will be sacrificed.

On the other hand, with joint optimization, the throughput can be obtained as $\lambda_{out}^{q=q^*, \lambda=\lambda^*} = 0.3607$ by combining (14) and (15). The performance loss is only 2%, i.e.,

$$1 - \frac{\lambda_{out}^{q=q^*, \lambda=\lambda^*}}{\lambda_{out}^*} = 2\%. \quad (17)$$

To evaluate the age performance gain brought by the optimal tuning, Fig. 4 shows how PAoI varies with n in the above three cases. It can be seen from Fig. 4 that with fixed setting, the PAoI exponentially increases with n , indicating that the age performance becomes intolerably low in massive access scenarios. In contrast, with either individual optimization or joint optimization, the PAoI A linearly grows with n . The performance gain becomes significant, especially when n is large or both the channel access probability q and the packet arrival rate λ can be dynamically tuned.

IV. CONCLUSION

This paper aims at optimizing the PAoI performance of slotted Aloha networks with FCFS service discipline by properly tuning the channel access probability and packet arrival rate of each sensor. Specifically, we obtain the closed-form expression of PAoI. Depending on whether the packet arrival rate can be

tuned or not, the individual optimization and the joint optimization are studied with the bi-stable behavior of the network being taken into consideration. In both cases, the optimal parameter setting and the corresponding minimum PAoI are explicitly characterized, and the throughput performance loss is further evaluated. The effect of the number of sensors on age performance is analyzed, which shows that the minimum PAoI with joint optimization increases linearly with network scale. Finally, simulations verify our results and show the notable gap in PAoI performance between joint optimization and individual optimization in the massive access case. Note that this paper focuses on slotted Aloha with FCFS discipline and finite buffer size, how to further optimize the PAoI of slotted Aloha with other queueing disciplines, such as last-come-first-served with preemption, and infinite buffer size is an interesting issue that deserves much attention in future work.

APPENDIX A PROOF OF THEOREM 2

To derive the optimal channel access probability and packet arrival rate for joint optimization, let us first obtain the optimal packet arrival rate $\lambda^*|_q$ when the access probability is fixed. According to (1) and (7), we have

$$\frac{\partial A}{\partial \lambda} = \frac{2nq}{(pq+\lambda)^2 - n\lambda pq^2} - \frac{1}{\lambda^2}, \quad (18)$$

$\lim_{\lambda \rightarrow 0} \frac{\partial A}{\partial \lambda} < 0$, and $\lim_{\lambda \rightarrow 1} \frac{\partial A}{\partial \lambda} \approx 2nq - 1$. Since $q^*|_{\lambda} > 1/2n$ according to (11), in the following, we only consider the $q > 1/2n$ case and therefore, $\lim_{\lambda \rightarrow 1} \frac{\partial A}{\partial \lambda} > 0$, implying that the optimal packet arrival rate should be in $(0, 1)$.

By assuming the network always operates at the desired steady-state point p_L , Lemma 1 presents the optimal packet arrival rate $\lambda_{p_L}^*$.

Lemma 1. *With $1/2n < q \leq 1$ and $p = p_L$, the minimum PAoI*

$$A^*|_{p=p_L} = \frac{nq \left(1 + \sqrt{1 + \frac{4}{nq}}\right) + 2}{2q \exp \left(- \frac{2}{1 + \sqrt{1 + \frac{4}{nq}}} \right)} - 1, \quad (19)$$

is achieved when the input rate

$$\lambda_{p_L}^* = \frac{2q \exp \left(- \frac{2}{1 + \sqrt{1 + \frac{4}{nq}}} \right)}{nq \left(1 + \sqrt{1 + \frac{4}{nq}}\right) - 2}. \quad (20)$$

Proof. By combining $\frac{\partial A}{\partial \lambda} = 0$ and (18), we have $(pq + \lambda)^2 - nq\lambda(pq + \lambda) - nq\lambda^2 = 0$, for which the single positive solution gives (20). \square

Note that with $1/2n < q \leq 1$ and $\lambda = \lambda_{p_L}^*$, the network may shift into the bi-stable region \mathcal{B} and therefore not operate at the desired steady-state point p_L . Fig. 5 illustrates the bi-stable region \mathcal{B} and mono-stable region \mathcal{M} . It can be seen

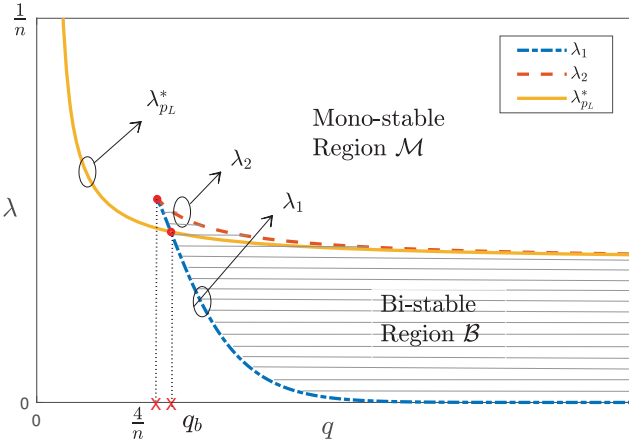


Fig. 5. Bi-stable region \mathcal{B} and mono-stable region \mathcal{M} .

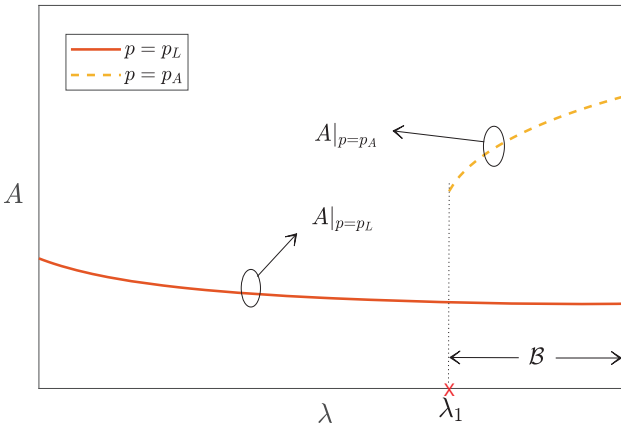


Fig. 6. PAoI A versus λ in bi-stable region \mathcal{B} and mono-stable region \mathcal{M} .

that $\lambda_{p_L}^*$ is included in mono-stable region \mathcal{M}_λ when $q < q_b$, where $q_b \approx \frac{4.51}{n}$ is the single non-zero root of equation

$$\exp\left(\frac{2\sqrt{1+\frac{4}{nq}}+2\sqrt{1-\frac{4}{nq}}}{\left(1-\sqrt{1-\frac{4}{nq}}\right)\left(1+\sqrt{1+\frac{4}{nq}}\right)}\right) = \frac{nq\left(1+\sqrt{1+\frac{4}{nq}}\right)-2}{nq\left(1-\sqrt{1-\frac{4}{nq}}\right)-2}, \quad (21)$$

which is derived by combining $\lambda_1 = \lambda_{p_L}^*$, (2) and (20).

When the channel access probability $1/2n < q \leq q_b$, the network is guaranteed to stay in mono-stable region \mathcal{M} and operate at the desired steady-state point p_L with the packet arrival rate $\lambda_{p_L}^*$, i.e.,

$$\arg \min_{\lambda} A|_{1/2n < q \leq q_b} = \lambda_{p_L}^*. \quad (22)$$

On the other hand, if $q > q_b$, then $(n, q, \lambda_{p_L}^*) \in \mathcal{B}$, implying that the network suffers from the risk of dropping to the undesired steady-state point p_A if $\lambda = \lambda_{p_L}^*$. To obtain the optimal arrival rate in this case, Fig. 6 depicts how the PAoI A varies with λ in bi-stable region \mathcal{B} and mono-stable region \mathcal{M} . It can be seen that when $\lambda \leq \lambda_1$, the network operates at the desired steady-state point p_L and the PAoI decreases as λ increases. As λ increases to $\lambda > \lambda_1$, the network goes in bi-stable region \mathcal{B} , and the PAoI will increase sharply if the network shifts to the undesired steady-state point p_A . Since the larger λ will increase the risk of the network shifting from p_L to p_A , in order to ensure the stable PAoI, the packet arrival

rate λ should be set to the boundary λ_1 to minimize the chance of operating at p_A , i.e.,

$$\arg \min_{\lambda} A|_{q \geq q_b} = \lambda_1, \quad (23)$$

and the corresponding PAoI can be obtained by substituting $\lambda = \lambda_1$ into (7).

Finally, the optimal packet arrival rate λ can be obtained as

$$\lambda^*|_q = \begin{cases} \frac{2q \cdot \exp\left(-\frac{2}{1+\sqrt{1+\frac{4}{nq}}}\right)}{nq\left(1+\sqrt{1+\frac{4}{nq}}\right)-2} & 1/2n < q \leq q_b, \\ \frac{2}{n\left(m-\frac{2}{nq}\right) \cdot \exp\left(\frac{2}{m}\right)} & q_b < q \leq 1, \end{cases} \quad (24)$$

by combining Lemma 1, (22) and (23), where $m = 1 - \sqrt{1 - \frac{4}{nq}}$, $q_b \approx \frac{4.51}{n}$, and p_1 is the non-zero root of the following equation.

$$p_1 = \exp\left(\frac{-n^2q\left(m-\frac{2}{nq}\right)\exp\left(\frac{2}{m}\right)}{2p_1q+n\left(m-\frac{2}{nq}\right)\exp\left(\frac{2}{m}\right)}\right). \quad (25)$$

For joint optimization, the channel access probability and the packet arrival rate should satisfy (11) and (24), which can be achieved if and only if $q = \frac{4\mathbb{W}_{-1}^2\left(-\frac{\sqrt{n\lambda}}{2}\right)}{n\left(-2\mathbb{W}_{-1}\left(-\frac{\sqrt{n\lambda}}{2}\right)-1\right)}$. The following Lemma 2 shows the optimal parameters of joint optimization $\{q^*, \lambda^*\}$.

Lemma 2. When the optimal channel access probability $q = \frac{4\mathbb{W}_{-1}^2\left(-\frac{\sqrt{n\lambda}}{2}\right)}{n\left(-2\mathbb{W}_{-1}\left(-\frac{\sqrt{n\lambda}}{2}\right)-1\right)}$, the joint optimization result $\{q^*, \lambda^*\}$ is given by

$$\begin{cases} q^* = \frac{2n\lambda^{*2}}{(p^*q^*+\lambda^*)^2-n\lambda^*p^*q^{*2}-\frac{2}{q^*}}, \\ \lambda^* = \frac{2}{n\left(m-\frac{2}{nq^*}\right) \cdot \exp\left(\frac{2}{m}\right)}, \end{cases} \quad (26)$$

where $m = 1 - \sqrt{1 - \frac{4}{nq}}$, and p^* denotes the successful transmission probability in (1).

Proof. When the channel access probability $q = \frac{4\mathbb{W}_{-1}^2\left(-\frac{\sqrt{n\lambda}}{2}\right)}{n\left(-2\mathbb{W}_{-1}\left(-\frac{\sqrt{n\lambda}}{2}\right)-1\right)}$, the packet arrival rate is λ_1 in (2) in order to ensure both (11) and (24) are satisfied. Let us solve the optimal channel access probability q^* first. According to (1) and (2), when $\lambda = \lambda_1$, the packet arrival rate λ and the successful transmission probability p are determined by q , and we have

$$\frac{\partial \lambda}{\partial q} = -\exp\left(\frac{-2}{1-\sqrt{1-\frac{4}{nq}}}\right) \cdot \left(\frac{1+\sqrt{1-\frac{4}{nq}}}{1-\sqrt{1-\frac{4}{nq}}}\right)^2, \quad (27)$$

$$\frac{\partial p}{\partial q} = \frac{-np^2q^2 \cdot \frac{\partial \lambda}{\partial q} - np\lambda^2}{(pq+\lambda)^2 - n\lambda pq^2}. \quad (28)$$

By combining (7), (27) and (28), the first-order differentiation $\frac{\partial A}{\partial q}$ can be obtained as

$$\begin{aligned} \frac{\partial A}{\partial q} = & -\exp\left(\frac{-2}{m}\right) \left(\frac{2-m}{m}\right)^2 \left(\frac{2nq}{(pq+\lambda)^2 - n\lambda pq^2} - \frac{1}{\lambda^2}\right) \\ & + \frac{2}{pq} \cdot \left(\frac{n\lambda^2}{(pq+\lambda)^2 - n\lambda pq^2} - \frac{1}{q}\right), \end{aligned} \quad (29)$$

where $m = 1 - \sqrt{1 - \frac{4}{nq}}$. It can be calculated that λ_1 exists if and only if $q \in [\frac{4}{n}, 1]$ by combining $\lambda_1 = \lambda_2$ and (2). We then have $\lim_{q \rightarrow \frac{4}{n}} \frac{\partial A}{\partial q} < 0$ and $\lim_{q \rightarrow 1} \frac{\partial A}{\partial q} > 0$. Therefore the single root of the equation $\frac{\partial A}{\partial q} = 0$ exists and the optimal channel access probability q^* can be solved by $\frac{\partial A}{\partial q} = 0$. The optimal packet arrival rate λ^* can be obtained by substituting q^* in (24). \square

Lemma 2 presents $\{q^*, \lambda^*\}$ in the form of strictly established equations, which is tricky to solve, so we will simplify it with approximation and notations. According to (26), q^* is the solution of the following equation.

$$\frac{2\alpha p n q^2 - 2n\lambda^2}{(pq+\lambda)^2 - n\lambda pq^2} - \frac{n\alpha p q^2 - 2n\lambda^2}{\lambda^2 q} = 0, \quad (30)$$

where $\alpha = \exp\left(\frac{-2}{1 - \sqrt{1 - \frac{4}{nq}}}\right) \left(\frac{1 + \sqrt{1 - \frac{4}{nq}}}{1 - \sqrt{1 - \frac{4}{nq}}}\right)^2$. Let $u = nq$, $f = n\lambda$, we have

$$f = \frac{2}{\left(1 - \frac{2}{u} - \sqrt{1 - \frac{4}{u}}\right) \cdot \exp\left(\frac{2}{1 - \sqrt{1 - \frac{4}{u}}}\right)} = g_1(u), \quad (31)$$

$$\alpha = \exp\left(\frac{-2}{1 - \sqrt{1 - \frac{4}{u}}}\right) \left(\frac{1 + \sqrt{1 - \frac{4}{u}}}{1 - \sqrt{1 - \frac{4}{u}}}\right)^2 = g_2(u). \quad (32)$$

It can be observed that f and α both are functions of u noted as $g_1(u)$ and $g_2(u)$ respectively. By the way, by substituting (31) in the fix-point equation in (1), the successful transmission probability p can be expressed as

$$p = \exp\left(\frac{g_1(u)u}{g_1(u) + pu}\right) = g_3(p, u). \quad (33)$$

It can be seen that (33) is an implicit function, and p is also determined by u . Finally by combining (31)-(33), (30) can be simplified as

$$2g_1g_3u^2 - 2g_1^2 = \left(\frac{g_2g_3u^3}{g_1^2} - 2u\right) \left((g_3 + \frac{g_1}{u})^2 - g_1g_3\right). \quad (34)$$

The solution of (34) can be approximately calculated as $u \approx 4.543$. Therefore the optimal channel access probability $q^* = \frac{u}{n} \approx \frac{4.543}{n}$ and the optimal packet arrival rate $\lambda^* = \frac{g_1(u)}{n} \approx \frac{0.4395}{n}$. The minimum PAoI can be obtained by combining (7) and (14).

REFERENCES

- [1] S. Kaul, R. Yates, and M. Gruteser, "Real-time status: How often should one update?" in *Proc. IEEE INFOCOM*, 2012.
- [2] Y. Sun and B. Cyr, "Sampling for data freshness optimization: Non-linear age functions," *IEEE J. Commun. Netw.*, vol. 21, no. 3, pp. 204–219, Jun. 2019.

- [3] H. Wu, C. Zhu, R. J. La, X. Liu, and Y. Zhang, "FASA: Accelerated S-ALOHA using access history for event-driven M2M communications," *IEEE/ACM Trans. Netw.*, vol. 21, no. 6, pp. 1904–1917, Dec. 2013.
- [4] W. Zhan and L. Dai, "Massive random access of machine-to-machine communications in LTE networks: Modeling and throughput optimization," *IEEE Trans. Wireless Commun.*, vol. 17, no. 4, pp. 2771–2785, Apr. 2018.
- [5] L. Dai, "Stability and delay analysis of buffered Aloha networks," *IEEE Trans. Wireless Commun.*, vol. 11, no. 8, pp. 2707–2719, Aug. 2012.
- [6] Z. Fang, J. Wang, J. Du, X. Hou, Y. Ren and Z. Han, "Stochastic optimization-aided energy-efficient information collection in Internet of Underwater Things networks," *IEEE Internet Things J.*, vol. 9, no. 3, pp. 1775–1789, Feb. 2022.
- [7] S. K. Kaul and R. D. Yates, "Status updates over unreliable multiaccess channels," in *Proc. IEEE ISIT*, pp. 331–335, Jun. 2017.
- [8] B. Yu, Y. Cai, and Dan Wu, "Joint access control and resource allocation for short-packet-based mMTC in status update systems," *IEEE J. Sel. Areas Commun.*, vol. 39, no. 3, pp. 851–865, Mar. 2021.
- [9] D. C. Atabay, E. Uysal, and O. Kaya, "Improving age of information in random access channels," in *Proc. AoI Workshop in conj. with IEEE INFOCOM*, July 2020.
- [10] O. T. Yavacan and E. Uysal, "Analysis of slotted ALOHA with an age threshold," *IEEE J. Sel. Areas Commun.*, vol. 39, no. 5, pp. 1456–1470, May 2021.
- [11] Y. H. Bae and J. W. Baek, "Age of information and throughput in random access-based IoT systems with periodic updating," *IEEE Wireless Commun. Lett.*, vol. 11, no. 4, pp. 821–825, April 2022.
- [12] X. Chen, K. Gatsis, H. Hassani, and S. Bidokhti, "Age of information in random access channel," in *Proc. IEEE ISIT*, Aug. 2020.
- [13] Z. Jiang, B. Krishnamachari, S. Zhou, Z. Niu, "Can decentralized status update achieve universally near-optimal age-of-information in Wireless multiaccess channels?" in *Proc. 30th Inte. Teletraffic Congr.*, vol. 01, pp. 144–152, Oct. 2018.
- [14] Y. Inoue, H. Masuyama, T. Takine and T. Tanaka, "A general formula for the stationary distribution of the age of information and its application to single-server queues," *IEEE Trans. Inf. Theory*, vol. 65, no. 12, pp. 8305–8324, Dec. 2019.
- [15] A. Maatouk, S. Kriouile, M. Assaad, and A. Ephremides, "The age of incorrect information: A new performance metric for status updates," *IEEE/ACM Trans. Netw.*, vol. 28, no. 5, pp. 2215–2228, Oct. 2020.
- [16] R. D. Yatesp, Y. Sun, D. R. Brown III, S. K. Kaul, E. Modiano, and S. Ulukus, "Age of information: An introduction and survey," *IEEE J. Sel. Area Comm.*, vol. 39, no. 5, pp. 1183–1210, May 2021.
- [17] W. Zhan and L. Dai, "Access delay optimization of M2M communications in LTE networks," *IEEE Wireless Commun. Lett.*, vol. 8, no. 6, pp. 1675–1678, Dec. 2019.
- [18] G. T. R. W. 69b R2 102340, "Smart grid traffic behaviour discussion," Apr. 2020.
- [19] Z. Wang and V. W. S. Wong, "Optimal access class barring for stationary machine type communication devices with timing advance information," *IEEE Trans. Wireless Commun.*, vol. 14, no. 10, pp. 5374–5387, Oct. 2015.
- [20] R. Talak, S. Karaman and E. Modiano, "Optimizing information freshness in wireless networks under general interference constraints," *IEEE/ACM Trans. Netw.*, vol. 28, no. 1, pp. 15–28, Feb. 2020.